J|A|C|S ARTICLES

Published on Web 02/04/2009

A Spectroscopic Study of Nicotine Analogue 2-Phenylpyrrolidine (PPD) Using Resonant Two-Photon Ionization (R2PI), Microwave, and 2D NMR Techniques

Danielle E. Martin, Evan G. Robertson,* Jonathan G. MacLellan, Peter D. Godfrey, Christopher D. Thompson, and Richard J. S. Morrison

School of Chemistry, Monash University, Victoria 3800, Australia

Received October 10, 2008; E-mail: Evan.Robertson@sci.monash.edu.au

Abstract: Conformational preferences of the nicotine analogue 2-phenylpyrrolidine (PPD) have been studied in both gaseous and solution phases. Theoretical calculations at the MP2 and B3LYP levels point to 5−6 stable conformers which differ in three degrees of conformational freedom; torsion between the two rings, inversion at the pyrrolidine (PY) amine, and PY ring puckering, characterized using the Cremer−Pople definition for pseudorotation. Only one conformer has a trans arrangement between the amino hydrogen and the phenyl substituent. It is 6−8 kJ mol^{-1} more stable than the cis conformers, has a perpendicular ring arrangement, and puckers at the nitrogen atom—similar to structures reported for nicotine. Resonant two-photon ionization (R2PI) data, including hole burn spectra, indicate only one conformer is present in the free jet expansion, and band contour analysis suggests assignment to the trans conformer. Confirmation was provided by microwave spectroscopy. Fifty-seven lines measured in the 48−72 GHz region were assigned to 206 *b*-type transitions and fitted to yield rotational constants within 2 MHz of MP2 values predicted for the trans conformer. The solution-phase conformers of PPD were studied using 1D and 2D ^{1}H NMR spectroscopy and solvent-based theoretical calculations. In marked contrast to the gas phase, NMR data reveals only cis conformers present in solution. Calculations confirm increased stability for these conformers when placed in simulated chloroform or water environments. Solvent molecules are believed to disrupt a crucial N···H(ortho) stabilizing interaction present within the trans conformer.

1. Introduction

Nicotine (Figure 1) is a commonly abused, addictive plant alkaloid whose effects on the human body are still under investigation. Although the negative repercussions are well-known, particularly in relation to tobacco use, there is potential for use of this drug as a therapeutic agent. Nicotine acts on the nicotinic acetylcholine receptors (nAChR), binding with particularly high affinity to the $\beta_4\alpha_2$ subtype predominantly found in the central nervous system.[1−5] These receptors play a crucial role in the processes of cognition, memory, and learning, and studies have shown that nicotine may actually benefit these processes in both animal and human models.[1−5] As such, nicotine has been the subject of numerous clinical trials involving a range of diseases, e.g., Alzheimer's,[2,3] Parkinson's,[3,6] schizophrenia,[3] and alcoholism.[7] Concurrent studies searching for comparable agonists without the detrimental side-effects are constantly improving our understanding of the nAChR binding site.

In the hunt for further agonists, models of the nAChR pharmacophore have been developed. As it is not currently possible to study the binding site of a receptor directly, pharmacophores provide valuable information regarding the structure of a receptor site. Pharmacophores discern the structural features of a molecule responsible for binding to a receptor site and producing a specific biological response.[8] Although the current model for the nAChR pharmacophore is still undergoing refinement, it is accepted that an effective pharmacophore requires both an onium and a hydrogen-bond acceptor site, and that the interatomic distance between these sites may influence binding affinity (see vector pharmacophore models as outlined by Glennon et al.[8]).[4,9] Nicotine is protonated under physiological conditions at the pyrrolidine (PY) nitrogen (Nsp^3)[8−10] and so has the onium and hydrogen-bond acceptor sites at the PY and pyridine nitrogens, respectively. The three-dimensional arrangement of these features also plays a crucial role. Molecular flexibility and interactions with surrounding

(1) Henningfield, J. E.; Fant, R. V. *Nicotine Tob. Res.* **1999**, *1*, S31–S35.
(2) Graton, J.; van Mourik, T.; Price, S. L. *J. Am. Chem. Soc.* **2003**, *125*, 5988–5998.
(3) Rezvani, A. H.; Levin, E. D. *Biol. Psychiatry* **2001**, *49*, 258–267.
(4) Cashin, A. L.; Petersson, E. J.; Lester, H. A.; Dougherty, D. A. *J. Am. Chem. Soc.* **2005**, *127*, 350–356.
(5) Elliott, R. L.; Ryther, K. B.; Anderson, D. J.; Raszkiewicz, J. L.; Campbell, J. E.; Sullivan, J. P.; Garvey, D. S.; Bioorg, *Med. Chem. Lett.* **1995**, *5*, 991–996.
(6) Quik, M.; Bordia, T.; O'Leary, K. *Biochem. Pharmacol.* **2007**, *74*, 1224–1234.
(7) Nixon, S. J.; Lawton-Craddock, A.; Tivis, R.; Ceballos, N. *Alcohol.: Clin. Exp. Res.* **2007**, *31*, 2083–2091.
(8) Glennon, R. A.; Dukat, M.; Liao, L. *Curr. Top. Med. Chem.* **2004**, *4*, 631–644.
(9) Seydou, M.; Gregoire, G.; Liquier, J.; Lemaire, J.; Schermann, J.-P.; Desfrancois, C. *J. Am. Chem. Soc.* **2008**, *130*, 4187–4195.
(10) Graton, J.; Berthelot, M.; Gal, J.-F.; Girard, S.; Laurence, C.; Lebreton, J.; Le Questel, J.-Y.; Maria, P.-C.; Naus, P. *J. Am. Chem. Soc.* **2002**, *124*, 10552–10562.

10.1021/ja807995n CCC: $40.75

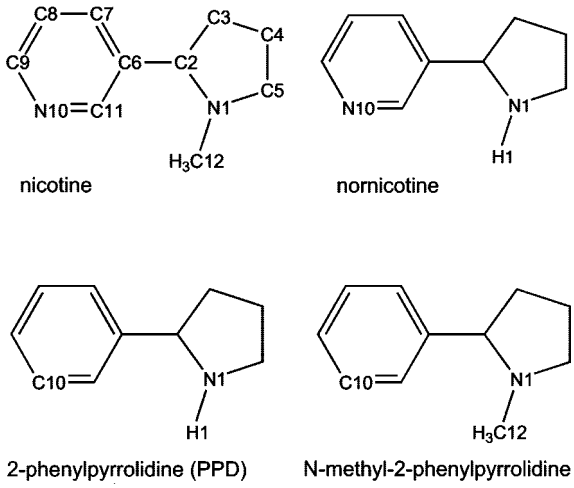

Figure 1. Structures of nicotine and selected analogues.

molecules, particularly with water, are known to influence pharmacophoric activity.[2,11] An improved understanding of molecular conformation can thus only aid rational drug design.

This paper focuses on gas- and solution-phase conformers of the nicotine analogue 2-phenylpyrrolidine (PPD). A subsequent paper will deal with *N*-methyl-2-phenypyrrolidine (MPPD) (see Figure 1). Both retain the key two-ring structural motif of nicotine but replace the pyridine with a phenyl group; PPD is closely related to nornicotine (found in tobacco along with nicotine), an analogue that displays slightly weaker binding affinity than nicotine itself.[8,12] Although removing the hydrogen-bond acceptor site at the pyridine nitrogen does significantly decrease the affinity of both PPD and MPPD for the nAChR,[5,8,12] it is hoped that study of these molecules will help to discern fundamental interactions influencing geometry. Structural elements, such as the relative positions of the ring systems, are likely to be preserved so that the phenyl and pyridyl compounds should be directly comparable.

Our group has recently been exploring the gas-phase conformers of small, bioactive molecules belonging to the $Ph(CH_2)_2X$ family.[13−18] Such molecules model a range of simple biological molecules by substitution of the functional group. Gas-phase experiments are a valuable alternative to as yet unfeasible in vivo experiments for determining the conformational preferences of bioactive molecules.

In this study, we compare the intrinsic (gas-phase) conformational properties of PPD with the conformation identified in organic solvent. Gas phase studies were conducted using resonant two-photon ionization time-of-flight (R2PI-TOF) spectroscopy and microwave jet spectroscopy, in conjunction with ab initio calculations. Solution phase behavior was examined using a series of 1D and 2D NMR technques including $^1H-^1H$ correlation spectroscopy (COSY) and $^1H-^1H$ nuclear Overhäuser effect spectroscopy (NOESY). Polarisable continuum model (PCM) and conductor-like screening model for real solvents (COSMO-RS) theoretical calculations were run in conjunction with NMR experiments.

2. Experimental Section

2.1. R2PI-TOF Spectroscopy. PPD was used as received from Fluorochem. The sample was heated to approximately 90 °C (363K), entrained in Argon carrier gas at 1.5 bar and pulsed into a vacuum chamber equipped with a time-of-flight mass spectrometer. One- and two-color R2PI experiments used frequency-doubled dye lasers in the wavelength region 260−267 nm, operating at 10 Hz. More complete descriptions of the R2PI equipment and laser systems have been reported previously.[17] For UV−UV hole burn (HB) spectroscopy, the probe laser was fixed to a specific wavelength corresponding to a spectral feature of interest. The burn laser was fired approximately 600 ns prior to the probe beam and scanned over wavelengths corresponding to the $\pi^* \leftarrow \pi$ transition region of the sample molecule while monitoring the ion signal from the probe laser.

2.2. Microwave Spectroscopy. A Stark-modulated millimeter-wave spectrometer was used to probe the low-energy rotational conformers of PPD in an unskimmed continuous free jet expansion. The sample was heated to ca. 55 °C (328 K) and seeded into a carrier stream of argon, with a flow rate of approximately 100 mL min^{-1}. The nozzle aperture was 1.0 mm in length and 0.3 mm in diameter. The rotational temperature of the sample after free jet expansion was approximately 5 K. The microwave absorption spectrum was first surveyed using a strip chart covering the 48−72 GHz range. Once a line was located, it was digitally recorded by repeat averaging of narrow band scans (2−5 MHz). Line frequencies were measured by least-squares fitting a Lorentzian function to each narrow band profile. Stark modulation relies on 33 kHz square-waves, generated by applying equal amplitude ground-clamped voltage waveforms of opposite polarity to parallel-plate electrodes separated by approximately 3.5 cm.

2.3. ^{1}H NMR Spectroscopy. NMR studies were performed on either a Bruker DRX400 or a Bruker DRX500 spectrometer. C_6D_6 and CD_3CN were dried over CaH_2 before being distilled and stored under N_2. Samples were prepared in a glovebox immediately prior to the experiments being performed. $CDCl_3$ was stored over K_2CO_3 and the sample was prepared without further purification. ^{1}H NMR (500 MHz, $CDCl_3$, 27 °C): δ 7.39 (d, 2H, *o*-Ph-H); 7.35 (t, 2H, *m*-Ph-H); 7.26 (t, 1H, *p*-Ph-H); 4.14 (t, 1H, H(2)); 3.24 (m, 1H, H(5a)); 3.04 (m, 1H, H(5b)); 2.22 (m, 1H, H(3b)); 2.08 (s, 1H, N−H(1)); 1.95 (m, 1H, H(4a)); 1.88 (m, 1H, H(4b)); 1.70 (m, 1H, H(3a)).

3. Results

3.1. Ab Initio. Ab initio calculations were performed using the Gaussian03 package.[19] PPD is a chiral molecule with a stereocenter at the C_2 atom. All structures presented are of *S* (also denoted (-)) configuration, related to the biologically active form of nicotine. The potential energy surface of PPD is quite complex, and so finding the full complement of conformers required a number of different strategies. Initial structures were identified at the semiempirical AM1 level using the HyperChem[20] conformational search engine. Further conformers were found using a series of B3LYP/6−31G(d) relaxed potential

(11) Amiri, S.; Sansom, M. S. P.; Biggin, P. C. *Protein Eng., Des. Sel.* **2007**, *20*, 353–359.
(12) Graton, J.; Berthelot, M.; Gal, J.-F.; Laurence, C.; Lebreton, J.; Le Questel, J.-Y.; Maria, P.-C.; Robins, R. *J. Org. Chem.* **2003**, *68*, 8208–8221.
(13) Robertson, E. G.; Thompson, C. D.; Morrison, R. J. S. *J. Chem. Phys.* **2004**, *121*, 12421–12427.
(14) Robertson, E. G.; Morrison, R. J. S. *Mol. Phys.* **2005**, *103*, 1625–1632.
(15) Martin, D. E.; Robertson, E. G.; Morrison, R. J. S. *Chem. Phys. Lett.* **2006**, *425*, 210–215.
(16) Martin, D. E.; Robertson, E. G.; Morrison, R. J. S. *J. Chem. Phys.* **2007**, *127*, 134307.
(17) Martin, D. E.; Robertson, E. G.; Thompson, C. D.; Morrison, R. J. S. *J. Chem. Phys.* **2008**, *128*, 164301.
(18) Robertson, E. G.; Martin, D. E.; Thompson, C. D.; Morrison, R. J. S.; Philis, J. G. *Chem. Phys. Lett.* **2008**, *463*, 29–32.
(19) Frisch, M. J.; et al. *Gaussian 03*; Gaussian, Inc.: Wallingford CT, 2004.
(20) *HyperChem*; Hypercube, Inc.: Gainesville, FL.

energy scans varying the different torsions and puckering within the PY ring, performed to ensure that no conformers had been overlooked.

Full ground-state optimizations were carried out using Hartree−Fock (HF/6−311G(d,p)), density functional (B3LYP/6−31G(d) and 6−311+G(d,p)), and Möller-Plesset second-order perturbation (MP2/6−311+G(d,p)) theories. From the initial 16 conformers identified at the AM1 level, relaxation processes reduced the number of stable conformers to eight at the B3LYP/6−31G(d) level, and to six at the B3LYP/6−311+G(d,p) level. A final five stable conformers were identified at the MP2/6−311+G(d,p) level, selected as appropriate for predicting conformational structures and energetic preferences where long-range interactions are involved.[16,22−24] Electronic states associated with $\pi^* \leftarrow \pi$ excitations of the phenyl ring were examined using configuration interaction singles (CIS) theory with a 6−311G(d,p) basis set. This level of theory has proven a reliable method for calculating the rotation of a $\pi^* \leftarrow \pi$ transition dipole moment (TDM) for phenyl derivatives such as PPD.[25−27] All results are summarized in Table 1 and Figure 2.

The potential energy minima vary in three degrees of conformational freedom. The first is a twisting of the two rings with respect to one another (characterized by the dihedral angle $\tau(H_2C_2C_6C_{11})$). The rings have a "perpendicular", i.e., $\tau(H_2C_2C_6C_{11}) \approx 0°$, or "parallel", i.e., $\tau(H_2C_2C_6C_{11}) \approx \pm 90°$, arrangement, and previous studies discussing nicotine identify a perpendicular arrangement between the PY and pyridine rings in the most stable conformers.[2,9,10,28−32] Parallel rings have so far only been observed for PPD; structure ^2E_Z in Figure 2 has a parallel arrangement between the two rings, with $\tau(H_2C_2C_6C_{11})$ equal to −84°.

The second degree of freedom concerns whether the amine hydrogen and the phenyl ring are both directed "up" with respect to the 5-membered ring (cis), or whether one is up and the other down (trans). These alternatives are denoted by the subscript labels *E* or *Z*, respectively. Only one conformer, the global minimum E_{1E}, has a trans arrangement. All remaining PPD conformers are cis.

The third degree of conformational freedom is pseudorotation within the PY ring, corresponding to changes in the puckering arrangement. This accounts for much of the structural differences between PPD conformers−the five stable conformers of PPD each show a different puckering about the PY cycle. To classify and label these conformers, we have calculated the pseudorotation angle (φ), and the puckering amplitude (*q)* parameters devised by Cremer and Pople.[21,33,34] Each structure is classified as either envelope (E), where one atom is out-of-plane relative to the other four ($\varphi \approx 0°$, 36°, 72°,...), or twist (T), where two atoms twist out-of-plane relative to the other three ($\varphi \approx 18°$, 54°, 90°...). Nomenclature incorporates the puckered atom and its position ($^+$ or $_-$) relative to the phenyl ring. This is illustrated for clarity in Figure S1 of the Supporting Information. Each of the five PPD structures predicted at the MP2 level have an envelope structure; E_{1E}, ^2E_Z, ^3E_Z, ^4E_Z, and ^5E_Z. Higher-energy twist conformers were observed at the lower B3LYP levels of theory (see Figure 2). The predominance of the envelope conformation follows a pattern identified by Pffafferott et al.,[33] where gaseous five-membered $(CH_2)_4X$ rings generally adopt envelope configurations when X has C_s symmetry. Conformer E_{1E} was favored at all levels of theory by approximately 5−6 kJ mol^{-1}. It is a trans conformer with a perpendicular arrangement between the two rings, and puckering at the nitrogen atom (pseudorotation angle 187°).

Table 1. Ab initio Calculated Molecular Properties of PPD in the Gas Phase

Conformer	E_{1E}	^2E_Z	^3E_Z	^4E_Z	^5E_Z
E_{rel} (kJmol^{-1})[a]	0.00	5.53	10.05	6.96	8.88
E_{rel} (kJ mol^{-1})[b]	0.00	7.03	9.81	6.53	8.36
E_{rel} (kJ mol^{-1})[c]	0.00	7.08	9.19	5.82	8.40
E_{rel} (kJ mol^{-1})[d]	0.00	6.58	5.57	5.61	6.44
E_{rel} (kJ mol^{-1})[e]	0.00	6.64	4.96	4.90	6.48
φ (deg)[d,f]	187.2	209.6	66.8	296.5	135.8
q (Å)[d,f]	0.45	0.39	0.42	0.42	0.38
$\tau(H_2C_2C_6C_{11})$[d]	16.5	−84.2	36.0	7.6	−7
$\tau(H_1N_1C_2C_6)$[d]	−68.4	52.2	−34.2	−9.5	28.1
$\tau(N_1C_2C_6C_7)$[d]	−41.5	−148.2	−23.0	−52.9	−68.2
$r(N-C_8)$ (Å)[d]	4.29	4.23	4.36	4.38	4.39
$r(N-C_{10})$ (Å)[d]	4.84	4.86	4.96	4.82	4.66
A'' (MHz)[d]	3052	3017	2492	2881	2488
B'' (MHz)[d]	622	657	753	658	659
C'' (MHz)[d]	591	556	680	612	616
μ_a (D)[d]	−0.78	−0.75	0.50	0.23	−0.23
μ_b (D)[d]	−0.84	1.11	0.42	0.62	1.71
μ_c (D)[d]	−0.41	−0.59	0.86	0.93	0.78
μ_{tot} (D)[d]	1.22	1.46	1.08	1.14	1.43
θ_{elec} (deg)[g]	12	19	20	−38	−44
TDM μ_a^2:μ_b^2:μ_c^{2g}	11:88:1	9:90:1	31:68:1	15:84:1	30:65:5
$\%\Delta A$[g]	−3.31	−1.71	−1.73	−4.01	−13.97
$\%\Delta B$[g]	0.15	−1.16	−1.19	1.30	11.85
$\%\Delta C$[g]	−0.73	−1.55	−1.31	−0.51	7.70

[a] B3LYP/6−31G(d). [b] B3LYP/6−311+G(d,p). [c] B3LYP/6−311+G(d,p) + zero-point correction. [d] MP2/6−311+G(d,p). [e] MP2/6−311+G(d,p) including B3LYP/6−311+G(d,p) zero-point correction. [f] The pseudorotational angle φ and puckering amplitude q, as defined by Cremer and Pople.[21] [g] S_1 properties calculated at CIS/6−311G(d,p) level. θ_{elec} and μ_a^2:μ_b^2:μ_c^2 refer to the S_1-S_0 TDM evaluated at the HF/6−311G(d,p) geometry. θ_{elec} is defined as the angle between the TDM alignment and the axis perpendicular to the benzene substituent (negative sign indicates clockwise movement toward the substituent). $\%\Delta A$, $\%\Delta B$, $\%\Delta C$ changes were evaluated by comparison of CIS and HF geometries.

3.2. R2PI Spectroscopy.

3.2.1. Survey Spectra. The one-color R2PI survey spectrum of PPD is displayed in Figure 3a, showing vibronic transitions near the $\pi^* \leftarrow \pi$ origin region for this molecule. Only one origin band is apparent, labeled band "X" at 37 537 cm^{-1}. The presence of just one conformer in the supersonic jet was confirmed by UV−UV HB spectroscopy. The HB spectrum shown in Figure

(21) Cremer, D.; Pople, J. A. *J. Am. Chem. Soc.* **1975**, *97*, 1354–1358.
(22) Robertson, E. G.; Simons, J. P. *Phys. Chem. Chem. Phys.* **2001**, *3*, 1–18.
(23) Carballeira, L.; Perez-Juste, I. *J. Chem. Soc., Perkin Trans.* **1998**, *2*, 1339–1345.
(24) Snoek, L. C.; Kroemer, R. T.; Hockridge, M. R.; Simons, J. P. *Phys. Chem. Chem. Phys.* **2001**, *3*, 1819–1826.
(25) Kroemer, R. T.; Liedl, K. R.; Dickinson, J. A.; Robertson, E. G.; Simons, J. P.; Borst, D. R.; Pratt, D. W. *J. Am. Chem. Soc.* **1998**, *120*, 12573–12582.
(26) Dickinson, J. A.; Hockridge, M. R.; Kroemer, R. T.; Robertson, E. G.; Simons, J. P.; McCombie, J.; Walker, M. *J. Am. Chem. Soc.* **1998**, *120*, 2622–2632.
(27) Selby, T. M.; Zwier, T. S. *J. Phys. Chem. A* **2005**, *109*, 8487–8496.
(28) Pitner, T. P.; Edwards, W. B.; Bassfeild, R. L.; Whidby, J. F. *J. Am. Chem. Soc.* **1978**, *100*, 246–251.
(29) Elmore, D. E.; Dougherty, D. A. *J. Org. Chem.* **2000**, *65*, 742–747.
(30) Takeshima, T.; Fukumoto, R.; Egawa, T.; Konaka, S. *J. Phys. Chem. A* **2002**, *106*, 8734–8740.
(31) Evain, M.; Felpin, F.-X.; Laurence, C.; Lebreton, J.; Le Questel, J.-Y. *Z. Kristallogr.* **2003**, *218*, 753–760.
(32) Muñoz-Caro, C.; Nino, A.; Mora, M.; Reyes, S.; Melendez, F. J.; Castra, M. E. *J. Mol. Struct. Theochem* **2005**, *72*, 113–122.
(33) Pfafferott, H. G.; Oberhammer, H.; Boggs, J. E.; Caminati, W. *J. Am. Chem. Soc.* **1985**, *107*, 2305–2309.
(34) Zubkov, S. V.; Chertkov, V. A. *Int. J. Mol. Sci.* **2003**, *4*, 107–118.

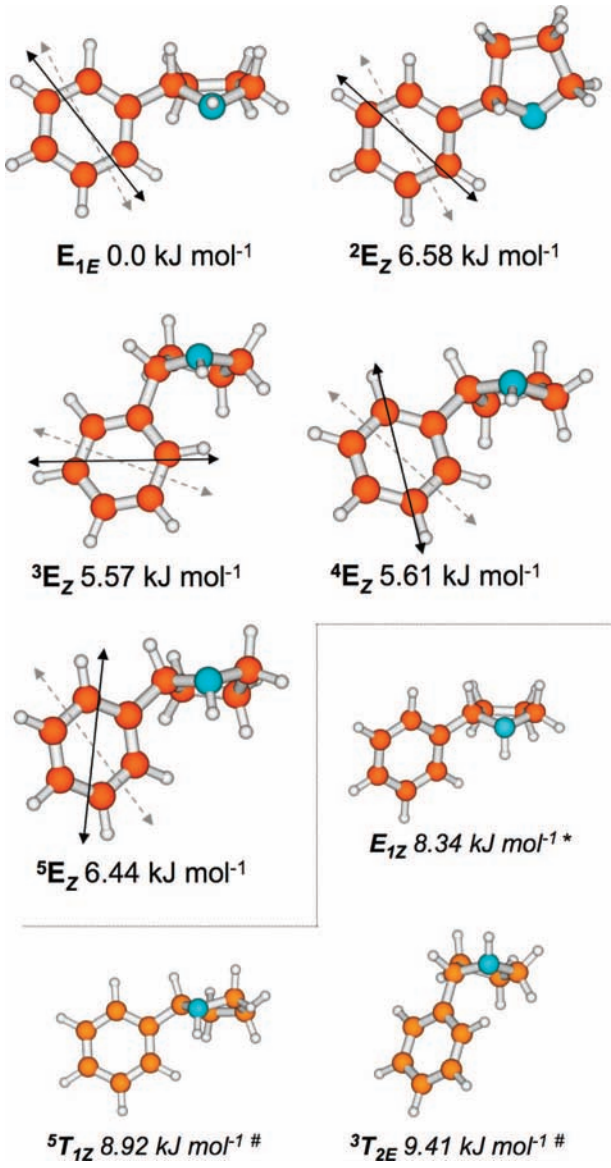

Figure 2. Molecular conformers and relative energies of PPD at the MP2/6−311+G(d,p) level of theory with predicted transition dipole moment (TDM) alignments for the $S_1 \leftarrow S_0$ transition. Smaller structures below the line relax at the MP2 level ($E_{1Z} \rightarrow {}^5E_Z$, ${}^5T_{1Z} \rightarrow {}^5E_Z$, ${}^3T_{2E} \rightarrow E_{1E}$), and consequently, their relative energies with respect to conformer E_{1E} are at the B3LYP/6−311+G(d,p) level (*) or at the B3LYP/6−31G(d) level (#).

3b was produced by probing the strong ring mode feature at 38 060 cm^{-1}. All observed vibronic features are accounted for, and thus originate from the same conformer. The excited-state lifetime of PPD was determined by measuring the two-color R2PI signal as a function of delay between the resonance excitation and nonresonance ionization lasers and fitting an exponential function to these data. The measured lifetime of 75 ns is comparable to the average 70 ns fluorescence lifetimes of most substituted benzenes.[16,17,35,36]

3.2.2. Rotational Band Contour Analysis. The rotational contour of band X, measured by two-color R2PI, is shown in Figure 4. Also shown are theoretical contours calculated for the five PPD conformers. The simulations were generated using rotational constants and transition dipole moments from the ab initio data, both of which vary considerably from one conformer to the next. For example, the $S_1 \leftarrow S_0$ transition dipole moment (TDM) alignments, shown in Figure 2, lie in the plane of the phenyl ring but are "rotated" (by an amount θ_{elec}) away from the axis perpendicular to the substituent by "through-bond" influences (largely via torsion about C_2C_6) and "through-space" interactions between aromatic and side-chain π- or lone-pair orbitals.[25] Rotational constants affect the sub-band spacing of the contours, and in the case of conformer ${}^5E_Z$ give rise to a simulation with an unusual shape that results from inertial axis switching between the S_0 and S_1 states.

Experimental band contour X shows predominant *b*-type rotational structure, similar to that observed for conformers E_{1E}, ${}^2E_Z$ and ${}^4E_Z$. Conformers ${}^3E_Z$ and ${}^5E_Z$ display more *a/b*-hybrid character. The spacing of Q-sub-bands in band X allows the value of $A'' - {}^1/_2(B'' + C'')$ to be estimated at 0.0805 cm^{-1}. Comparison with computed values for each conformer: 0.0816 cm^{-1} (E_{1E}), 0.0804 cm^{-1} ($2E_Z$), 0.0592 cm^{-1} (${}^3E_Z$), 0.0749 cm^{-1} (${}^4E_Z$) and 0.0617 cm^{-1} (${}^5E_Z$), favors conformer E_{1E} or ${}^2E_Z$. The E_{1E} simulation is most similar in appearance to band X and relative energies support this assignment. Conformer E_{1E} is ~5 kJ mol^{-1} more stable than any of the other conformers at the MP2/6−311+G(d,p) level.

3.2.3. Vibronic Analysis. The R2PI spectra in Figure 2 show several vibronic features whose shifts from the origin, X, reflect vibrational spacings in the excited S_1 state. Table S1 in the Supporting Information displays the CIS/6−311G(d,p) vibrational frequencies and assignments for the S_1 state of PPD conformer E_{1E}. Theoretical frequencies are in excellent agreement when compared to observed band positions, listed relative to the origin at 37 537 cm^{-1}. Features typical of a phenyl derivative include a low frequency torsional mode about the C_2-C_6 bond at 48 cm^{-1} and a strong 6b ring mode at a shift of 523 cm^{-1}. Weak PY ring modes including a C_5 and a N_1 pucker are also observed, as is a relatively strong bending mode $\delta(C_2C_6C_{11})$ at a shift of 319 cm^{-1}.

3.2.4. Microwave Spectroscopy. Microwave jet spectroscopy has been used to analyze the ground-state rotational structure of PPD in the gaseous phase. A total of 57 lines were detected in the 48−72 GHz range. All could be assigned to μ_b and μ_c type transitions of a single asymmetric rotor molecule. μ_a lines could not be detected as they originate from rotational levels with high J values that are very weakly populated within this spectral region. Measured transitions spanned J values from 9 to 27, and K_a values 4−12. Lines with $K_a'' \geq 6$ were quadruply degenerate; $K_a'' = 5$ lines showed double degeneracy for $J'' \geq 22$. At $K_a'' = 4$, lines were singly degenerate such that b- and c-type lines could be resolved with the b-dipole component shown to be larger than the c-component. Microwave lines were fitted to Watson's *S*-reduced Hamiltonian using H. M. Pickett's software.[37] A total of 206 transitions including degenerate sets were fitted with a rms error of 0.04 MHz. Table 2 lists the constants derived from this fit, together with MP2 rotational constants for conformer E_{1E}. The agreement is excellent, better than ±2 MHz. The corresponding constants for the remaining conformers (see Table 1) are sufficiently different that they may be eliminated from consideration. B3LYP centrifugal distortion constants from a rovibrational calculation are of similar magnitude to the moderately well determined experimental

(35) Martinez, S. J.; Alfano, J. C.; Levy, D. H. *J. Mol. Spectrosc.* **1993**, *158*, 82–92.
(36) Martinez, S. J.; Alfano, J. C.; Levy, D. H. *J. Mol. Spectrosc.* **1991**, *145*, 100–111.
(37) Pickett, H. M. *J. Mol. Spectrosc.* **1991**, *148*, 371–377.

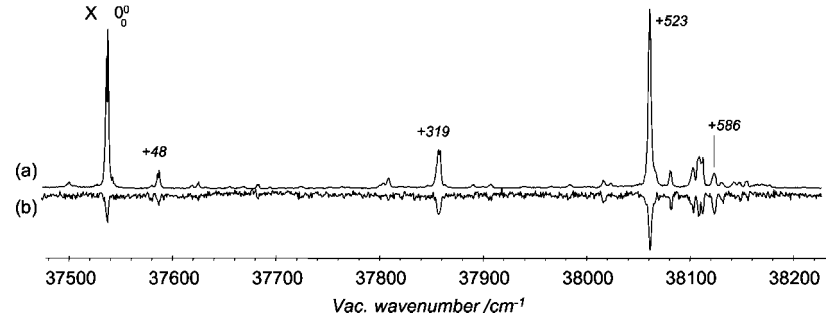

Figure 3. (a) One-color R2PI spectra of PPD, monitoring the PPD^+ mass channel and (b) the associated UV−UV hole burn (HB) spectrum, obtained by probing the intense ring mode feature at 38 060 cm^{-1}. Strong vibronic features are labeled with their shift relative to the origin band.

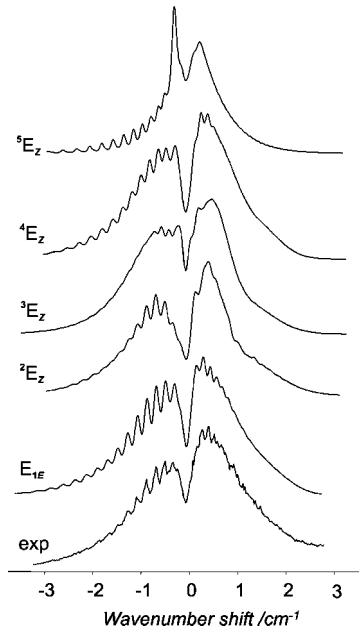

Figure 4. Predicted rotational band contours for theoretical PPD conformers ^5E_Z, ^4E_Z, ^3E_Z, ^2E_Z, E_{1E}, and the R2PI experimental band contour of PPD measured at origin band "X" 37 537 cm^{-1} (bottom trace). Simulation parameters are listed in Table 1: Rotational constants A'', B'', C''; changes in rotational constants upon excitation $\%\Delta A$, $\%\Delta B$, $\%\Delta C$; hybrid band character $\mu_a^2:\mu_b^2:\mu_c^2$; $T_{rot} = 8$ K and HWHH = 0.06 cm^{-1}.

Table 2. Fitted Microwave Constants for PPD using Watson's *S*-Reduced Hamiltonian

conformer	obsd	E_{1E}
A'' (MHz)[a]	3051.1590(13)	3052
B'' (MHz)[a]	624.1132(28)	622
C'' (MHz)[a]	589.9782(21)	591
D_J (kHz)[b]	−0.02527(77)	0.0232
D_{JK} (kHz)[b]	−0.0890(47)	0.0685
D_K (kHz)[b]	0.2966(79)	0.4242
d_1 (kHz)[b]	0	−0.00008195
d_2 (kHz)[b]	0.000215(45)	0.0008198
no. of lines measured	57	
no. of lines fitted	206	
rms residual	0.04	
J_{max}	26	
K_a range	5−12	

[a] MP2/6−311+G(d,p). [b] B3LYP/6−311+G(d,p).

values. The Supporting Information includes a complete set of transitions (Table S2) and examples of spectral line profiles (Figure S2).

3.2.5. ^{1}H NMR Spectroscopy. The solution phase structure of PPD has been established by a series of 1D and 2D homonuclear NMR experiments, including ^{1}H, ^{1}H−^{1}H-COSY, and ^{1}H−^{1}H-NOESY studies in conjunction with gas and solution phase calculations. The general applicability of this assignment has been confirmed by spectra run in three deuterated solvents; $CDCl_3$, CD_3CN and C_6D_6. The $CDCl_3$ spectra are most helpful as proton resonances show isolated signals for all nonequivalent protons. As the two ortho- and the two meta-phenyl protons show only one resonance each, both sets must be equivalent (or exchanging), at least on the NMR time scale. Variable-temperature studies in dry CD_3CN, ranging from the freezing point of the solvent to the boiling point (−42 to 80 °C), did not instigate separation of these aryl resonances.

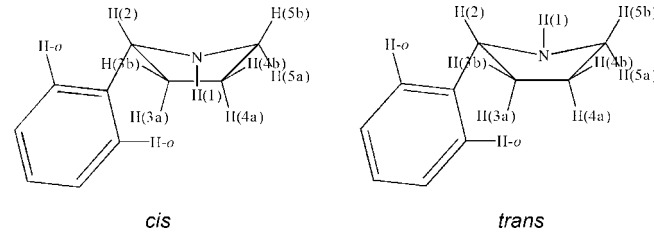

Figure 5. Structural representations of the PPD envelope cis-E_{1Z} and trans-E_{1E} diastereomers, showing proton designations.

The magnitude of a NOE enhancement is proportional to the inverse of the ^{1}H−^{1}H internuclear distance, r, to the power six ($1/r^6$).[38] A comparison of the observed NOEs to the calculated interproton distances for all stable conformers should therefore allow the preferred conformer in a specific solution to be identified. In deuterated chloroform six NOE crosspeak resonances are observed: H(*o-Ph*)···H(1), H(*o-Ph*)···H(2), H(*o-Ph*)···(H3), H(1)···H(5a), H(2)···H(3b), and H(2)···H(5b). The labeling of these protons is shown in Figure 5, the spectrum in Figure 6, and full proton assignments in all three solvents in Tables S3−S5 of the Supporting Information.

First we consider the three (*o*-H)···PY-H(*x*) crosspeaks. Comparison of the shortest calculated *o*-H···PY-H distances for the MP2 predicted gas phase conformers (see Table S6a in the Supporting Information) shows the closest fit for this model is trans conformer E_{1E}—the most stable conformer in the gas phase. All five predicted conformers show similar distances to these protons, whereas the remaining four conformers have at least one other distance within a comparable range (<2.7 Å) and are therefore expected to produce additional NOEs. However, the observation of an NOE for the amine proton H(1) to H(5a) and the absence of cross peaks to H(5b) or H(2) indicates a cis conformation. It is therefore evident that the trans conformer E_{1E} is not observed in solution. The cis diastereomer

(38) Bell, R. A.; Saunders, J. K. *Can. J. Chem.* **1970**, *48*, 1114–1122.

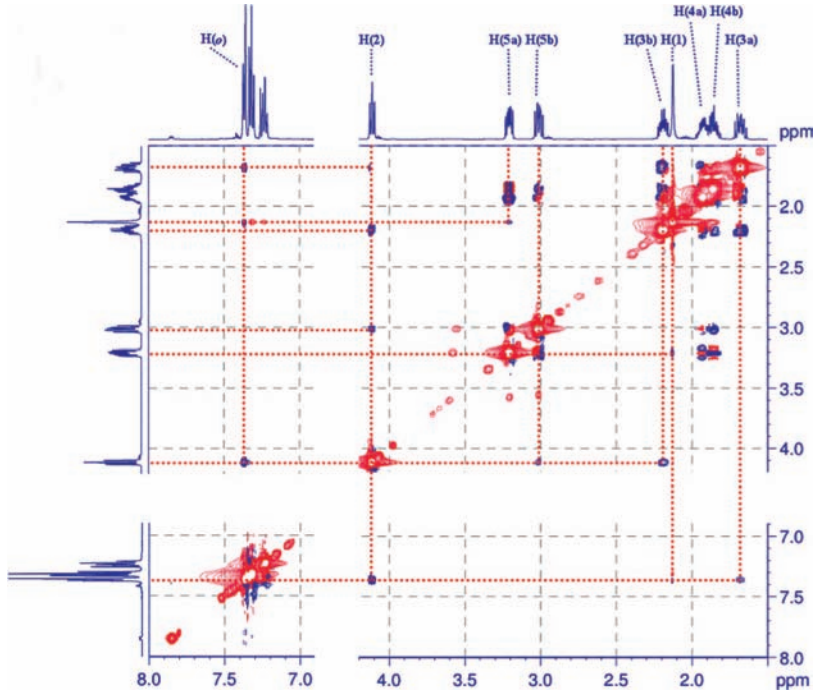

Figure 6. ^{1}H−^{1}H-NOESY spectrum of PPD in $CDCl_3$, showing regions 1.5−4.2 and 6.9−8.0 ppm. The absence of a signal at (1.70, 4.14) suggests that the weak feature at the complementary position (4.14,1.70) is a noise artifact, rather than evidence of an H(2)···H(3a) interaction.

Table 3. Ab initio Calculated Molecular Properties of PPD in Solution

	conformer (gas)											
	E_{1E}		E_{1Z}		^2E_Z		^3E_Z		^4E_Z		^5E_Z	
solvent	$CHCl_3$	H_2O	$CHCl_3$	H_2O	$CHCl_3$	H_2O	$CHCl_3$	H_2O	$CHCl_3$	H_2O	$CHCl_3$	H_2O
conformer (solution)	E_{1E}	E_{1E}	E_{1Z}	$^2T_{1Z}$	$^2T_{1Z}$	^2E_Z	^3E_Z	^3E_Z	^4E_Z	^4E_Z	^bE_Z	$^5T_{1Z}$
E_{rel} (kJmol^{-1})[a]	0.00	0.00	5.06	2.61	5.92	5.10	5.53	5.06	5.70	5.05	5.16	3.59
E_{rel} (kJmol^{-1})[b]	0.00	0.00	4.24	3.05	5.22	3.75	4.71	5.22	5.28	4.46	5.77	1.74
E_{rel} (kJmol^{-1})[c]	0.00	0.00	4.20	0.83	5.76	0.68	4.70	4.35	4.49	4.32	3.38	1.85
E_{rel} (kJmol^{-1})[d]	0.00	0.66	3.39	1.94	5.05	0.00	3.88	5.40	3.80	4.39	3.52	0.66
E_{rel} (kJmol^{-1})[e]	0.00	0.00	2.46	2.01	3.46	4.23	6.63	3.26	5.06	4.59	2.29	2.06
E_{rel} (kJmol^{-1})[f]	0.32	0.54	0.00	0.00	5.16	4.18	6.52	3.96	4.27	3.81	0.47	0.66
φ (deg)[d,g]	186.7	186.7	173.6	202.7	203.8	207.4	65.1	66.0	297.0	295.0	146.6	161.0
μ_{tot} (D)[d]	1.58	1.85	1.83	1.98	1.82	2.12	1.32	1.46	1.46	1.70	1.83	2.11

[a] PCM B3LYP/6−311+G(d,p). [b] PCM B3LYP/6−311+G(d,p) + Gibbs thermal energy correction. [c] PCM MP2/6−311+G(d,p). [d] PCM MP2/6−311+G(d,p) including PCM B3LYP/6−311+G(d,p) Gibbs thermal energy correction. [e] COSMO-RS MP2/6−311G(d,p)//CPCM MP2/6−311+G(d,p). [f] COSMO-RS MP2/6−311+G(d,p)//CPCM MP2/6−311+G(d,p). [g] The pseudorotational angle φ and puckering amplitude q, as defined by Cremer and Pople.[21]

E_{1Z} is stable at the B3LYP level of theory but is energetically unfavorable (E_{rel} = +8.3 kJ mol^{-1}) and at the higher MP2 level E_{1Z} relaxes to form conformer ^5E_Z. Regardless, a look at the inter H distances of this conformer (see Table S6a−c in the Supporting Information) shows that it provides a better correlation to the data given by the ^{1}H-^{1}H-NOESY spectrum than conformer E_{1E}.

Evidently the gas and solution phase conformations of PPD are different, and the gas phase calculations are not suitable for assignation of the solution state structure. Consequently, PCM and COSMO-RS//CPCM theoretical calculations in chloroform at the B3LYP and MP2 levels were performed, using B3LYP/6−311+G(d,p) gas-phase conformers as starting structures. Calculations were also conducted in water (nature's solvent) for comparison. Relative energies and structural parameters are listed in Table 3 (and Table S7 in the Supporting Information). Inter H distances at the PCM MP2/6−311+G(d,p) level are presented in Table S8a−c in the Supporting Information.

PCM and COSMO-RS relative energies show a drastic change to that reported in the gas phase. In both chloroform and water environments at the PCM level, the relative energies of the cis conformers decrease by ∼2−4 kJ mol^{-1} when compared to that predicted in the gas phase. Conformer E_{1Z} in particular is now stable at the MP2 level of theory, and relative stabilities increasingly favor the cis conformers E_{1Z} and ^5E_Z at the higher levels of theory. At the COSMO-RS/MP2/6−311+G** level, conformer E_{1Z} is actually preferred in both solvents to conformer E_{1E}, and the relative energy of conformer ^5E_Z is only 0.5 kJ mol^{-1} in $CHCl_3$ and 0.7 kJ mol^{-1} in H_2O. Clearly, solvent interactions play a significant role in stabilizing the different conformers. There are also structural changes associated with the solvent environment. For example, the parallel arrangement of the two rings shown by conformer ^2E_Z in the gas phase and in chloroform, is altered in the simulated water environment. The rings twist and become perpendicular, as evidenced by the change in $\tau(H_2C_2C_6C_{11})$ from 93.1° in $CHCl_3$ to −4.7° in H_2O, and this increases the relative stability of the conformer. Other

structural changes, for example, in pseudorotational angles to produce twist (T) structures, are minor and do not significantly alter the structural parameters from those observed in the gaseous phase.

Analysis shows that the inter H distances of conformer E_{1Z} best fit the NOESY spectrum, although it should be stated that NMR experiments provide a time averaged view of interactions occurring in solution. On the basis of these results, it cannot be ruled out that two or more energetically similar conformers are undergoing interconversion. In the gas phase there is virtually no energetic barrier between E_{1Z} and ^5E_Z conformers. It is therefore feasible that conformer ^5E_Z is also present in solution, and this conformer would produce a very similar NOESY spectrum. However, if ^5E_Z were present, an additional NOE from H(1) to H(4a) would be expected as the H(1)···H(4a) calculated distance in ^5E_Z is 2.66 Å. As this NOE is not observed, the conformer present in solution is believed to be E_{1Z}. Again, it could be argued that if the conformers are interchanging, particularly if the population of ^5E_Z is less than that of E_{1Z}, the additional interaction from ^5E_Z may not be strong enough to be observed. Variable-temperature and NMR parameter studies may be able to resolve this more satisfactorily but such studies were beyond the scope of this investigation.

To check that the E_{1Z} conformational preference was not merely a $CDCl_3$ solvent-dependent aberration, we performed analogous experiments in the more polar solvent CD_3CN and in the aromatic solvent C_6D_6 (see the Supporting Information). An unambiguous conformational assignment was not possible from either solvent directly but the data obtained in both cases strongly supports the presence of the cis conformer E_{1Z}.

4. Discussion

4.1. Conformational Preferences in the Gaseous Phase. The conformational landscape of PPD is surprisingly complex, given that it is a small molecule comprising just two linked rings. Much of this complexity results from puckering within the five-membered PY ring that gives rise to many potential minima, though the precise number varies with level of theory. Experimentally however, just one conformer (E_{1E}) is observed. In energetic terms this conformer is the clear winner by a margin of more than 5 kJ mol^{-1} according to theoretical calculations at the MP2/6−311+G(d,p) level. The stability of conformer E_{1E} may be rationalized by considering the intrinsic preferences of the PY ring and the interactions between the two rings.

Two stable conformers have been identified for the unsubstituted PY.[39] Both have an envelope conformation puckered at the nitrogen; one has an axial N−H bond and the other has an equatorial one. The millimeter-wave spectroscopic study by Caminati et al.[39] demonstrated that the equatorial form was more stable, resolving doubt from past experimental and theoretical studies. More recently Carballeria et al.[40] showed that theoretical parameters calculated for the five-membered ring are highly dependent upon the level of theory and basis set used. In general, larger basis sets are required to correctly predict a preference for the equatorial PY conformer, with the best theoretical estimate for the axial/equatorial energy difference being about 80−100 cm^{-1} (∼1 kJ mol^{-1}).

The axial conformer of PY is present in the E_{1Z} conformer of PPD, although this conformer is found at the B3LYP levels of theory only. At the MP2 level, E_{1Z} relaxes into conformer ^5E_Z, believed to be due to destabilizing interhydrogen interactions between the axial N−H and the phenyl ring (NH···H(ortho), 2.44 Å, C_3H···H(ortho), 2.42 Å). The equatorial conformer of PY is present in the stable E_{1E} conformer of PPD. Importantly, conformer E_{1E} benefits from a stabilizing interaction between the "lone pair" electron density on the nitrogen atom and an ortho hydrogen atom of the phenyl ring; the equivalent interaction energy of ammonia and benzene has been estimated[41] at 6 kJ mol^{-1}, which would largely account for the stability of conformer E_{1E}. The N···H(ortho) distance of PPD is 2.63 Å and the orientation is fairly optimal. The only other conformer with a geometry that allows this interaction is conformer ^2E_Z (and $^3T_{2E}$, though this is a PE minima at the B3LYP/6−31G(d) level only and relaxes to E_{1E} at higher levels). The "parallel" rings in conformer ^2E_Z, however, where $\tau(H_2C_2C_6C_{11})$ is −84° and $\tau(C_3C_2C_6C_7)$ is 153°, place atom C_3 very near the plane of the phenyl ring and result in a destabilizing, short interhydrogen C_3H···H(ortho) distance of 2.38 Å. This repulsion counteracts the attractive N···H(ortho) interaction such that conformer ^2E_Z is over 6 kJ mol^{-1} higher in energy than conformer E_{1E}, which has a more favorable near-perpendicular dihedral of $\tau(C_3C_2C_6C_7) = -105°$. In general, the optimal dihedral angle $C_\beta C_\alpha C_{ipso} C_{ortho}$ for an alkyl chain attached to a phenyl group is ±90° as in ethylbenzene, or ±60° when the chain is branched such that there are two β-carbons.[42] Although the remaining PPD conformers share the optimal perpendicular ring arrangement of E_{1E}, they lack the crucial N···H(ortho) attraction. A similar CH···Nsp^3 interaction is important in stabilizing the Nsp^2 protonated form of nornicotine in the gas phase.[10]

4.2. Conformational Flexibility and Relaxation. The ability of nicotine and related analogues to flex and adopt an optimal shape for receptor binding is important in the biological context, and barriers to conformational interconversion influence this flexibility. Similarly, barriers affect the number of conformers observed in a gaseous free jet expansion. Studies by Ruoff et al.[43] and Brown et al.[44] show that barriers above 400−800 cm^{-1} (5−10 kJ mol^{-1}) are sufficient to prevent conformational relaxation in the free jet. A notional potential energy (PE) scheme for the different conformers of PPD is shown in Figure 7; barrier heights are calculated from relaxed PE scans at the B3LYP/6−311+G(d,p) level. Interconversion involves various combinations of the three degrees of freedom described earlier: inter-ring torsion, inversion at the amine and pseudorotation. The largest barriers at ∼8 kJ mol^{-1} for $^4E_Z \rightarrow E_{1E}$ and ∼7 kJ mol^{-1} for $^3E_Z \rightarrow E_{1E}$, involve amine (cis−trans or *Z*−*E*) inversion coupled to pseudorotation. Pseudorotation shifts the PPD conformers through consecutive envelope and twist structures to convert between cis and trans structures while bypassing the high barrier associated with direct inversion.[40] Moving between ^2E_Z and E_{1Z} (barrier 3 kJ mol^{-1}) requires inter-ring twisting, again coupled to pseudorotation. For those conversions that involve mainly pseudorotation in the absence of other rearrangements, they have only low barriers to

(39) Caminati, W.; Dell' Erba, A.; Maccaferri, G.; Favero, P. G. *J. Mol. Spectrosc.* **1998**, *191*, 45–48.
(40) Carballeira, L.; Perez-Juste, I.; Van Alsenoy, C. *J. Phys. Chem.* **2002**, *106*, 3873–3884.
(41) Weyers, K.; Freudenberg, T.; Ritze, H.-H.; Radlo, W.; Stert, V. *Z. Phys. D* **1997**, *39*, 217–223.
(42) (a) Borst, D. R.; Joireman, P. W.; Pratt, D. W.; Robertson, E. G.; Simons, J. P. *J. Chem. Phys.* **2002**, *116*, 7057–7064. (b) Seemann, J. I.; Secor, H. V.; Breen, P. J.; Grassian, V. H.; Bernstein, E. R. *J. Am. Chem. Soc.* **1989**, *111*, 3140–3150.
(43) Ruoff, R. S.; Klots, T. D.; Emilsson, T.; Gutowsky, H. S. *J. Chem. Phys.* **1990**, *93*, 3142–3150.
(44) Godfrey, P. D.; Brown, R. D.; Rogers, F. M. *J. Mol. Struct.* **1996**, *376*, 65–81.

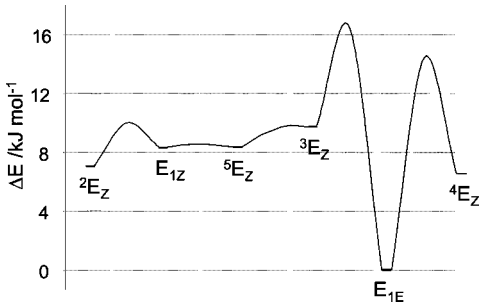

Figure 7. Notional potential energy surface (PES) of PPD, at the B3LYP/6−311+G(d,p) level. Separate relaxed scans varied $H_2C_2C_6C_{11}$ (5° steps), $N_1C_2C_3C_4$ (2° steps), and $H_1N_1C_5C_4$ (2.5° steps).

conversion, e.g., <1 kJ mol^{-1}, and at the MP2 level, there is virtually no barrier preventing E_{1Z} from relaxing to ^5E_Z. Given these relative energy differences, it is likely that some population of cis conformers are initially present in the free jet expansion. The barriers to amine inversion are of intermediate magnitude such that relaxation could be inhibited; however, the absence of an R2PI signal from any conformer other than E_{1E} suggests that *Z*−*E* relaxation does occur.

4.3. Conformational Preferences in the Solution Phase. Conformational equilibrium is determined by a number of different factors and can be phase-dependent. In the gaseous state, conformation is determined by intramolecular interactions including steric and electrostatic influences. In solution, a balance develops between these intramolecular interactions and intermolecular interactions with the local environment, though this will not necessarily result in a conformational change. If a phase change were to cause an associated change in the charge state of a molecule, e.g., zwitterion formation, then conformational changes would be expected. A neutral molecule, however, is not assumed to undergo major conformational shifts, particularly when moved between the gaseous state and an organic solvent of low polarity. Nicotine, for example, maintains a trans structure in both the solution phase and the gas phase[2,9,28,32,45] and this behavior is considered typical for most neutral molecules. Nevertheless, it should not be presumed that all flexible molecules will behave in the same way, and PPD presents a prime example.

NMR experiments, supported by PCM and COSMO-RS calculations in chloroform or water, show that the most populated conformer of PPD in solution is the cis conformer E_{1Z}, as opposed to the trans conformer E_{1E} identified in the gas phase. Although unusual, such a conformational mismatch between the different phases is not unprecedented and has previously been documented for other flexible molecules.[46,47] A good example is the biphenyl molecule, which alters conformation depending on the phase.[46] As a solid, the rings of biphenyl are coplanar; in the liquid phase, the rings twist to give a torsional angle between 30°−40°; in the gas phase, the angle is measured at 45°. Intermolecular interactions with the local environment obviously influence molecular stability.

In the case of PPD, solvent molecules are believed to disrupt the stabilizing interactions occurring within conformer E_{1E}, primarily the N···H(ortho) interaction previously discussed. Gas phase ab initio calculations on E_{1E}·$CHCl_3$ and E_{1Z}·$CHCl_3$ clusters, bound via a weak CH···N H-bond, show that as with the solvent calculations, the cis−trans energy difference is drastically reduced (MP2 1.4 kJ mol^{-1}, B3LYP 1.9 kJ mol^{-1}). The bound chloroform molecule appears to disrupt the N···H(ortho) interaction of the trans conformer E_{1E}; the distance between the PY-N and the nearest ortho-H increases from 2.63 Å in the monomer to 3.57 Å as the molecule readjusts to accommodate the bulky chloroform. Without this interaction the stability of the E_{1E} monomer is drastically reduced. It is therefore feasible that cis conformers could dominate in solution.

4.4. Comparisons to Nicotine and Nornicotine. Numerous theoretical and experimental studies focusing on gas-,[2,10,12,29,30] solution-,[9,28,32,45,48] and solid-phase[31] nicotine have been reported in the literature. Two stable trans stereoisomers have been identified. Each show a trans configuration between the pyridine and *N*-methyl substituents, and neutral monomers contain PY in an envelope conformation puckered at the nitrogen. This arrangement is directly comparable to conformer E_{1E} of PPD. The two rings are also roughly perpendicular in orientation; the stereoisomers differ by ∼180° at the $\tau(H_2C_2C_6C_7)$ dihedral. Theoretical studies for nicotine also identify potential cis conformers.[29,30] They are sterically less stable and are considered unlikely to be observed experimentally; NMR analysis indicates that nicotine exists at a ratio of 10:1 trans:cis in trifluoroacetic acid solution,[45] whereas ab initio theory predicts the cis conformers of nicotine are ∼9 kJ mol^{-1} less stable than the trans.[9,32]

Nicotine shows a high degree of molecular rigidity.[2,10,11] Graton et al.[10] find a large 110 kJ mol^{-1} barrier to torsion between the two rings (C_2−C_6) at the HF/6−31G(d,p) level, which hinders interconversion between the two trans isomers. This barrier is reduced to 25 kJ mol^{-1} in nornicotine, as a consequence of removing the bulky methyl group that hinders ring rotation.[10] The magnitudes of these barriers may be overestimated (it is not clear from the text whether these are relaxed or rigid PE scans, and the level of theory is modest) but the trend is clear. PPD, like nornicotine, has a comparatively low barrier. A relaxed PE scan rotating the C_2−C_6 torsion in conformer E_{1E} shows an energy barrier of ∼16 kJ mol^{-1} (MP2/6−311+G(d,p) level). As a consequence, PPD and nornicotine are able to more freely interconvert between PE minima. Nicotine also appears to be more constrained with respect to pseudorotational PY puckering; only cis conformers puckered at the nitrogen have been identified, although it should be noted that nicotinic studies do not systematically explore pseudorotational variation about the PY ring. In comparison, PPD displays increased molecular flexibility. Up to five stable cis structures have been identified by theory, each puckering at a different atom in the PY ring.

As stated earlier, the pharmacophoric relevance of the internitrogen distance of nicotine and its influence over binding affinity is still being explored. Numerous nAChR ligands show a range of interatomic distances[8] broadly ranging between 4.5 and 6.5 Å. Epibatidine, for example, is a potent analgesic with an internitrogen distance[8] of 5.5 Å, whereas in the endogenous neurotransmitter acetylcholine (ACh), the distance between the quaternary ammonium nitrogen and carbonyl oxygen is only 4.96 Å.[30,32] Nicotine itself has two stereoisomers traditionally labeled "A" (or I) and "B" (or II), such that the *r*(N−N) for A (4.89 Å) is greater than *r*(N−N) for B (4.27 Å).[30] In the past,

(45) Whidby, J. F.; Seeman, J. I. *J. Org. Chem.* **1976**, *41*, 1585–1590.
(46) Celebre, G.; De Luca, G.; Mazzone, G. *J. Mol. Struct., Theochem* **2005**, *728*, 209–214.
(47) (a) Cossé-Barbi, A.; Massat, A. *Struct. Chem* **1994**, *5*, 37–41. (b) Celebre, G.; Cinacchi, G.; De Luca, G.; Giuliano, B. M.; Iemma, F.; Melandri, S. *J. Phys. Chem. B* **2008**, *112*, 2095–2101.
(48) Bikádi, Z.; Simonyi, M. *Curr. Med. Chem.* **2003**, *10*, 2611–2620.

conformer A has been considered most likely to be the physiologically active form,[10,29,30] largely on the basis of the longer N−N separation. Bikádi and Simonyi[48] identified two dihedral angles that may also contribute to the binding affinity of nAChR agonists: $\tau_1(N_1C_2C_6C_{11})$ and $\tau_2(C_2C_6C_{11}N_{10})$. They examined a range of cholinergic agents at the AM1 level and found that binding affinity may be improved by a τ_2 dihedral close to 180° (which is always the case for aromatic derivatives such as PPD) and τ_1 dihedral between −80 and −140°. Curiously, they then quote a τ_1 value for gaseous *S*-nicotine of +136.2°. Although this angle corresponds to nicotine conformer A, a subsequent X-ray crystallographic study has shown that it is nicotine conformer B that binds to acetylcholine binding protein (AChBP), a substitute for nAChR.[49] Examination of the published structure reveals that twenty crystallographically distinct nicotine molecules have an average τ_1 of around −73° (angles range from −51 to −79°), and an average r(N−N) of 4.4 Å. In PPD conformer E_{1E} (gas phase), the equivalent $\tau_1(N_1C_2C_6C_7)$ and $r(N_1-C_8)$ parameters corresponding to nicotine conformer B are −41.5° and 4.29 Å at the MP2 level. These values should be considered reasonably accurate given the close agreement between calculated and observed rotational constants. The corresponding values for conformer E_{1Z} in solution are −64° and 4.40 Å in chloroform; −59° and 4.40 Å in water (see PCM MP2/6−311+G(d,p) data in Table S7 of the Supporting Information). The solution-phase parameters in particular are in good accord with those reported for nicotine. It is interesting to note that for both nicotine and PPD, the N···N distance and τ_1 angles are outside the values currently considered optimal for binding affinity.

5. Conclusion

The conformation of PPD in the gas phase has been examined using a combination of R2PI and microwave spectroscopy. Just one conformer was found to be present in the supersonic free jet, and its assignment to trans conformer E_{1E} is strongly supported by ab initio calculations at the B3LYP and MP2 levels. Calculations also predict a number of cis conformers, each around 6−8 kJ mol^{-1} less stable than trans conformer E_{1E}. Conformers differ with respect to three degrees of freedom; torsion between the two rings (C_2-C_6), inversion at the PY amine, and pseudorotation within the PY ring.

The conformational preferences of PPD in solution were also examined using 1D and 2D ^{1}H NMR spectroscopy. Experiments were run in the deuterated solvents C_6D_6, $CDCl_3$, and CD_3CN and covered a range of polarities. Results were supported by PCM and COSMO-RS theoretical calculations in chloroform and in water, and together yielded unexpected results. A pronounced change in the conformational stabilities of cis and trans conformers was observed and rationalized between the gas- and solution-phases. Solvent effects appear to disrupt crucial stabilizing interactions within the trans E_{1E} conformer and cis conformer E_{1Z} (and potentially conformer ^5E_Z) is present in solution instead. This change in conformational preference may have future implications. For example, the properties of chemicals in nonpolar organic solvents are often modeled using gas-phase ab initio calculations, and obviously in some cases, this may not be appropriate. PPD, however, is thought to present an unusual case in that a subtle balance of forces within the strained five-membered ring allow the conformation to change even through the weak intermolecular forces implied in low-polarity solvents.

One element that is preserved between gas-phase and solvated PPD is the strong conformational preference for perpendicular ring structures. This results in $r(N_1-C_8)$ distances that consistently fall within a 4.2−4.4 Å range. Although this distance is relatively fixed, the pseudorotational flexibility of the PY ring may actually assist nicotine derivatives such as nornicotine (which shows only slightly weaker binding affinity than nicotine itself[8,12]) to bind to the nAChR receptor site; applying the vector pharmacophore model,[8] the molecule can direct a H-bond at a variety of angles within the receptor site. In direct contrast, nicotine maintains its trans structure in both the gas and solution phases and is considered a fairly rigid molecule. The methyl group appears to confer a more strongly defined energetic predisposition for the trans arrangement at the PY ring, and we are presently exploring the effects of this additional methyl group by complementary gas and solution phase studies of *N*-methyl-2-phenylpyrrolidine (MPPD). As this is a structurally closer analogue to nicotine, analysis of this molecule should improve overall comparisons.

Acknowledgment. Financial support from the Australian Research Council and from Monash University is gratefully acknowledged. Quantum chemistry calculations were carried out using the Australian Partnership for Advanced Computing (APAC) National Facility. The authors also thank Dr. Ekaterina Izgorodina for her advice with the solution-based theoretical calculations, Hypercube Inc. and Dr. Laszlo Jicsinszky for writing and supplying the HyperPucker program used to calculate the Cremer-Pople ring puckering parameters, Tony Robertson for adapting the puckering program for our purposes, and Dr. Peter J. Nichols and Dr. Roger J. Mulder for their work on the NMR experiments at Monash University and CSIRO-MHT (Molecular and Health Technologies), respectively.

Supporting Information Available: Figures S1 and S2, Tables S1−S8, and complete author list for ref 19. The tables include assignments of vibronic features; detailed microwave spectroscopy data; ^{1}H NMR assignments in C_6D_6, $CDCl_3$ and CD_3CN; and ab initio data such as interproton distances for the most stable conformers of PPD. This material is available free of charge via the Internet at http://pubs.acs.org.

JA807995N

(49) Celie, P. H. N.; van Rossum-Fikkert, S. E.; van Dijk, W. J.; Brejc, K.; Smit, A. B.; Sixma, T. K. *Neuron* **2004**, *41*, 907–914.